Effect of elastic scattering in the Earth on cold dark matter experiments

J. I. Collar and F. T. Avignone III
Department of Physics and Astronomy, University of South Carolina, Columbia, South Carolina 29208
(Received 22 October 1992)

The diurnal modulation of fluxes and velocity distributions of cold dark matter (CDM) candidate particles, due to elastic scattering on the constituent nuclei of the Earth, is predicted. The geology, nuclear physics, the Earth's orientation, rotation, and trajectory through the galactic halo are included as well as the isotropic Maxwellian velocity distribution of CDM in the rest frame of the galactic halo. Observable modulations in detection rates and energy spectra are predicted for some interesting theoretical and experimental scenarios. The effects are seen to be maximal at southern latitudes. The differences in the sensitivity of experiments at southern and northern latitudes are explored. It is shown that it would be possible to detect Dirac neutrinos with densities well below those heretofore experimentally excluded.

PACS number(s): 95.35.+d, 14.60.Gh

I. INTRODUCTION

The fascinating question of what types of matter constitute the approximately 90% of the Universe unobservable by optical and radio astronomy has created an interesting marriage between astronomy, astrophysics, elementary particle physics, and cosmology. The first realization of this "missing mass" problem occurred almost 60 years ago [1]. There are a number of comprehensive reviews in the literature [2,3] covering the early developments, and more recent overviews updating the subject [4–6]. There is now a large body of evidence that this "dark matter" must exist [2–7] to explain the dynamics of galaxies, clusters of galaxies, and in fact galaxy formation.

One of the most important questions embedded in this subject is the nature of the dark matter (DM) itself. An accurate theoretical prediction, or a correct educated hypothesis based on indirect evidence, could inspire the successful search for DM. Popular candidates are weakly interacting massive particles (WIMP's), massive light neutrinos or axions, Jupiters, brown dwarfs, black holes, or other massive astrophysical compact halo objects (MACHO's), quark nuggets, strongly interacting massive particles (SIMP's), etc. Such candidates are broadly characterized as cold dark matter (CDM), heavy nonrelativistic particles, or hot dark matter (HDM) in the form of relativistic light neutrinos. CDM can be baryonic or nonbaryonic, and the various hypotheses for DM can be constrained indirectly by astrophysics and by cosmology. The ratio of the density of baryonic matter to the critical closure density, Ω_b, is constrained by big bang nucleosynthesis [5], for example, while the fraction of DM that must be cold is constrained by large scale structure through the density fluctuations required for galaxy formation.

A major breakthrough in our understanding of this large scale structure and strong evidence favoring, or perhaps confirming, big bang nucleosynthesis, was announced recently based on the data from the differential microwave radiometer on board the Cosmic Background Explorer (COBE) satellite [8–10]. Reference [10] discusses the various DM models consistent with the observed fluctuations in the cosmic microwave background radiation. The general conclusion is that the observed background fluctuations are "consistent with a number of models of structure formation."

These models involve mixtures of baryonic DM, hot and cold nonbaryonic DM, vacuum energy, as well as various values of the Hubble constant. The data do not uniquely fit all parameters, but models that propound a mixture of different kinds of dark matter are in best agreement with the observations. Accordingly, experimental bounds that depend on the assumption that there is only a single component to the local halo density (whose estimated value is in itself subject to a large degree of uncertainty) may be unrealistic. This notion engendered our earlier Letter [11] on the subject which was based on the school of thought generally confirmed by the COBE data.

Direct experimental searches for CDM started with ultralow background ionization detectors [12–14]; however, the basic ideas go back to the work of Drukier and Stodolsky [15] and that of Goodman and Witten [16]. The underlying physical principle involves coherent scattering of long wavelength CDM particles from nuclei. In Ref. [15], the recoil energy of the nucleus changes a small superconducting sphere in a magnetic field from a superconducting to a normal state, producing a detectable change in magnetic moment. In ionization detectors, this recoil energy produces a large number of charge-hole pairs that are collected, producing a pulse proportional to the recoil energy.

There are a number of detection schemes under development [17], for example: tunnel-junction detectors [18], superconducting spheres and arrays [19], phonon bolometers [20], and a new and very interesting combination bolometer-ionization detector [4]. The major common problem with all direct detection techniques is that they will always have some level of background; therefore, a claim of direct detection would not be possible unless the detector clearly discriminates between pulses due to nuclear recoil and those due to photons, charged particles,

and mechanical vibrations. Even with 100% reliability of identifying nuclear recoil pulses it would be difficult to unambiguously claim direct observation without resorting to some unique feature of the CDM signal that distinguishes it from the background.

The purpose of this paper is to present in some detail the method and results of the calculations briefly discussed in our previous Letter [11], pertaining to one such unique signature of CDM. The calculations evaluate the effects of elastic scattering of CDM on the constituent nuclei of the Earth on detection rates at northern and southern latitudes. For some values of the coupling constant and particle masses, we predict considerable diurnal modulations in count rates and energy spectra that are maximum for latitudes at about 30° to 40° south. Such modulations could be used to support a claim of direct detection that would be ascertained by the variation of the effect with the geographical location of the detector and time of day.

It is most important that in principle the exploitation of this effect is not dependent on the detection technique. Any of the techniques listed above would be enhanced in sensitivity by searching the data for daily modulation, with the caveat that the magnitude of the effect depends on mass and coupling strength.

The fundamental notion of analyzing direct search data to detect modulations was developed earlier by Drukier, Freese, and Spergel [21], by Freese, Frieman, and Gould [22], and by Spergel and Press [23]. These authors calculated the effects on detection rates and energy spectra due to the annual modulation of the relative velocity of the Earth and the galactic halo. The impact of this effect on counting rates depends on energy thresholds of the detectors involved and on background but can produce a predictable modulation of 4–6%. Presently operating WIMP detectors are just reaching the stability and low levels of short lived backgrounds ($T_{1/2} \leq 1$ yr) to produce data of the quality that these modulations can be searched for [24]. The advantage of their technique is that WIMP's with coupling constants and masses too small to be affected by scattering in the Earth can still have their energies changed enough to produce an annual modulation of counting rates. The diurnal modulations discussed herein are stronger and easier to unveil; however, they would only be measurable for some of the interesting regions of the mass-coupling constant plane.

II. DETECTION RATES

The rate of detection of WIMP's that leave energy $E_{\rm dep}$ in the detector can be expressed as [12]

$$R_{E\rm dep} = Nn \lim_{\Delta T \to 0} \left\{ \Delta T \int_{V_{\rm min}(m_\delta)}^{V_{\rm max}} f(v) v \frac{d\sigma}{dT} dv \right\} , \quad (1)$$

where T is the recoil energy of the target nucleus, $f(v)$ is the speed distribution of the CDM, N is the total number of target nuclei, n is the number density of CDM particles of mass m_δ, and $d\sigma/dT$ is the differential scattering cross section given below. The measured deposited energy $E_{\rm dep}$ and the nuclear recoil energy T are connected by a relative efficiency factor (REF) discussed in earlier papers [12–14]. The quantity $V_{\rm min}(m_\delta)$ is the minimum relative velocity that can leave $E_{\rm dep}$, and $V_{\rm max}$ is the maximum velocity of WIMP's relative to the detector and is the sum of the galactic escape velocity and the velocity of the Earth through the halo. The differential cross section for WIMP's with vector couplings to Z^0 bosons and that scatter from nuclei by Z^0 exchange is given by [12]

$$\frac{d\sigma}{dT} = \frac{G^2}{8\pi} \frac{M_R^2}{T_{\rm max}} [Z(1-4\sin^2\theta_W) - N]^2 \times \exp(-2M_N T R^2/3\hbar^2) , \quad (2)$$

where G is the effective coupling constant, M_R is the reduced mass, $T_{\rm max}$ is the maximum nuclear recoil energy of the target nucleus of mass M_N, and R is its radius. Z and N are the number of protons and neutrons in the target nucleus, respectively, and θ_W is the weak mixing angle. The exponential is a form factor that accounts for the decrease in cross section caused by the loss in coherence of the scattering process with the increase in linear momentum of the CDM relative to the target nuclei. This factor must be included in all theoretical predictions of the cross sections and detection rates. Failure to do so will lead to unrealistically high predicted detection rates.

The coupling constant G is the Fermi weak coupling constant arbitrarily scaled: for example,

$$G^2 = G_F^2 \left[\frac{G_f}{G_W} \right]^2 , \quad (3)$$

where for heavy left-handed Dirac neutrinos $G_f = G_W$, while for neutral technibaryons $(G_f/G_W)^2 \approx 10$, and for sneutrinos $(G_f/G_W)^2 \approx 2$. Spin-dependent and -independent scattering mechanisms have recently been proposed for a range of neutralino candidates [25–27], with cross sections between one and three orders of magnitude smaller than those for Dirac neutrinos.

III. DAILY ECLIPSING OF CDM BY THE EARTH

Earlier we showed that for an interesting range of CDM masses and coupling constants, coherent elastic scattering from nuclei in the mantle and the core of the Earth can produce a modulation of counting rates and energy spectra possibly observable in some experiments [11]. We performed a number of Monte Carlo calculations to determine the entry points on Earth as well as the initial velocities of CDM particles according to their distribution in the frame of the Earth. Then we followed the trajectories through the Earth while accounting for the possibility of scattering, in order to determine the exit points and final velocities.

The CDM particles are assumed to obey a Maxwell-Boltzmann distribution in the frame of the halo of the form

$$p(v)dv = \text{const} \times v^2[\exp(-3v^2/2V_{\text{disp}}^2)]dv \ , \qquad (4)$$

where the dispersion velocity $V_{\text{disp}} = 270 \pm 25$ km sec^{-1}. The distribution is truncated at the value of v equal to the galactic escape velocity, $V_{\text{esc}} = 500$ to 650 km sec^{-1}. We used the lower value of this velocity, which will lead to conservative predictions for the effects of scattering in the Earth. The model parameters used here are those suggested by Freese, Frieman, and Gould [22]. The speed distribution of Eq. (4) is isotropic in the frame of the halo. Velocities selected as random variables using Eq. (4) must be added vectorially to the negative of the velocity of the Earth through the halo in order to obtain the correct distribution in the frame of the Earth. The annual average of the velocity of the Earth through the halo along $\hat{\mathbf{V}}$ was taken from Mihalas and Binney [28]. This speed varies from about 245 km sec^{-1} in December to about 275 km sec^{-1} in June [22]. In of all our calculations except where explicitly stated, we use the commonly accepted DM halo density of 0.4 GeV per cubic centimeter [22].

The geometry of the problem is best described by two geocentric polar coordinate systems (Fig. 1). The polar axis of one is the unit vector $\hat{\mathbf{V}}$ of the velocity of the center of the Earth through the halo. The polar axis of the other, $\hat{\mathbf{Z}}$, is the Earth's axis of rotation. The angle θ specifies members of an infinite set of "isodetection rings." The azimuthal symmetry about $\hat{\mathbf{V}}$ dictates that the CDM flux and velocity distribution will be the same anywhere on a given isodetection ring, hence the name.

As the Earth rotates about $\hat{\mathbf{Z}}$, a detector located at a given point on it will rotate through many values of θ, and hence the counting rate and velocity distribution will be modulated according to how much the elastic scattering of the WIMP's on nuclei in the mantle and core affects their exit points and velocities. This will depend on their masses and coupling constants.

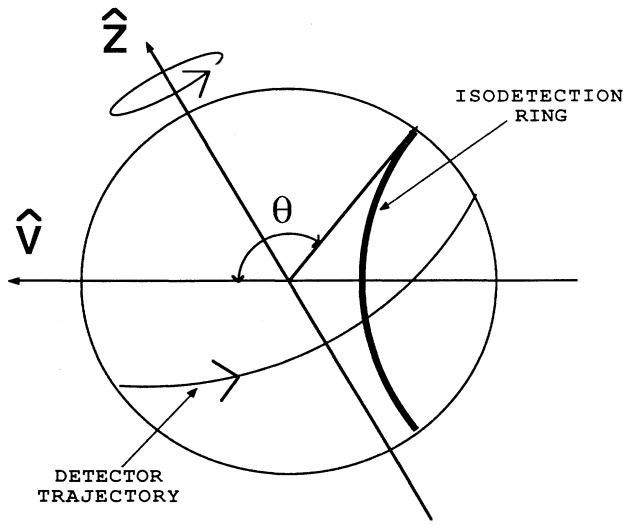

FIG. 1. Geometry of the calculation showing the velocity of the Earth through the galactic halo $\hat{\mathbf{V}}$, the Earth's axis of rotation $\hat{\mathbf{Z}}$, and the isodetection rings on which the velocity distributions and fluxes are uniform.

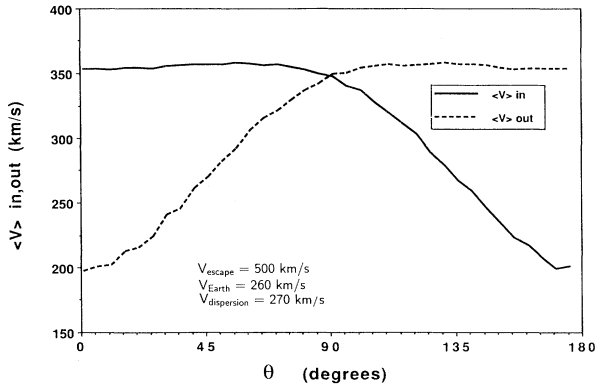

FIG. 2. The calculated average velocity of CDM particles into and out of the Earth in the absence of scattering. The angle θ is defined in Fig. 1.

The first step in the calculation is to determine the distributions of flux, speed, and direction of the incoming CDM particles on a selected set of isodetection rings; the rings were chosen at 1° intervals. The resulting average velocities of the incoming and outgoing particles in the absence of scattering are depicted in Fig. 2. Figure 3 shows a plot of the fluxes into and out of the Earth as a function of θ, also for the case when scattering in the Earth is not included.

The next step is to choose the incoming flux and velocity of a large number of trials and to follow the trajectory of each individual particle through the Earth as it scatters and loses energy. For this we model the Earth using current conventional wisdom of geology to construct the regions properly weighted in their constituent nuclei and to account for the continuous variation of the density with depth. Table I gives the depth of the boundary of the crust, mantle, inner core, and outer core, the percentage of the total mass that the region contains, the elements, and the average region densities [29–31]. The

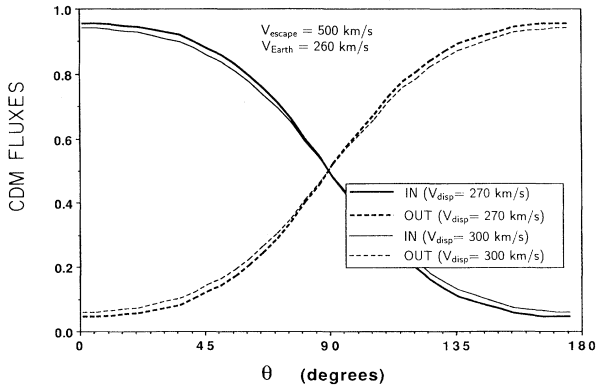

FIG. 3. The calculated fluxes into and out of the Earth in the absence of scattering, as a function of θ for two values of the dispersion velocity of the Maxwell-Boltzmann distribution of CDM in the halo. In the case of a "transparent" Earth, the sum of both fluxes is the same for all values of θ. This total flux has been normalized to unity here.

TABLE I. Elemental composition of the Earth's crust, mantle, and core. The crust has been neglected in our calculations due to its small thickness.

Region	Boundary depth (km)	% of mass	Components (% total mass)	$\langle\rho\rangle(10^3$ kg m$^{-3})$
Crust	~33	~1	O,Si,Al,Ca,Fe,Mg, Na,K	2.7
Mantle	~2885	68	O(30%),Si(15%), Mg(14%),Fe(6%), Ca(1.5%),Al(1.1%), Na(0.4%)	4.5
Outer core	~5000	29.3	Fe(25.2%),S(3.5%), Ni(0.6%)	11.8
Inner core	~6371	1.7	Fe(1.35%),Ni(0.35%)	15

particles are followed until they reach an exit point and the flux and velocity distributions of the exiting particles are calculated for the various isodetection rings. This allows us to construct the modified values of n and $f(v)$ in Eq. (1) for any value of θ. Figure 4 shows the anatomy of one sample calculation. In this calculation the particle mass was chosen with $m_\delta c^2=7$ GeV, and $(G_f/G_W)^2=1000$. The redistribution of exit points due to the "shadow" of the Earth's dense and iron-rich core is evident in that figure.

Plots of the normalized fluxes and mean velocities of CDM particles for masses between 3 GeV and 300 TeV, for various values of their coupling constants for coherent elastic scattering from nuclei, are shown in Figs. 5 and 6, respectively. The dependence of the detection rates on the latitude of the detector can be appreciated by reference to Fig. 7, which shows the angle θ plotted against the time in days after the vernal equinox of 1990 for several different geographical locations. These functions oscillate with a 24 h period; however, they undergo small changes in amplitude ($\sim 10\%$) with a periodicity of one tropical year. The reason for these is a variation in the relative angle between $\hat{\mathbf{V}}$ and $\hat{\mathbf{Z}}$ that results from the orbiting motion of the Earth: While $\hat{\mathbf{Z}}$ is essentially fixed in space, the direction of $\hat{\mathbf{V}}$ is determined by the vectorial sum of the Sun's velocity through the halo [28] ($|\mathbf{V}_{\rm Sun}|\cong 262\pm 25$ km/sec) and that of the Earth around the Sun ($|\mathbf{V}_{\rm Earth}|\cong 30$ km/sec), which changes continuously in direction through the year. This change in the direction of $\mathbf{V}_{\rm Earth}$ is also responsible for the annual modulation effect described in Refs. [21–23]. Details of these calculations can be found in a recent unpublished report [32]. However, the most relevant feature to be learned from Fig. 7 is that most locations in the northern hemisphere are only able to scan values of θ smaller than 90° at any given time of the year. Of the examples shown in that figure, it is clear that a detector in southern Australia will experience the maximum change in detection rates. An equivalently effective latitude in the Americas lies near Buenos Aires, Argentina. While Figs. 5 and 6 are convenient for demonstrating the effect and its dependence on geographical location, they do not constitute a

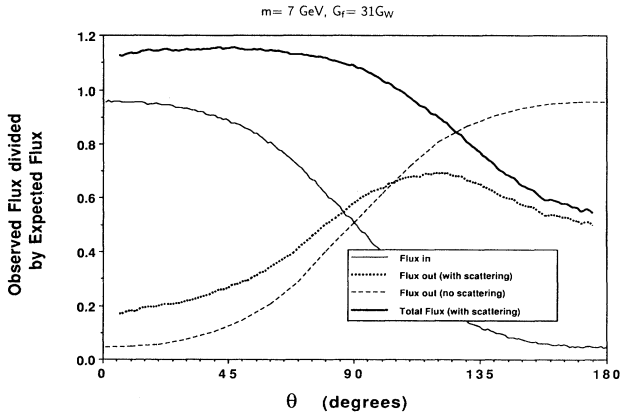

FIG. 4. Comparison of the fluxes into and out of the Earth without scattering, with the flux out and total flux with elastic scattering in the Earth. The chosen mass was $m_\delta c^2=7$ GeV with a coupling constant $(G_f/G_W)^2=1000$. All fluxes have been divided by the expected or total flux in the absence of scattering.

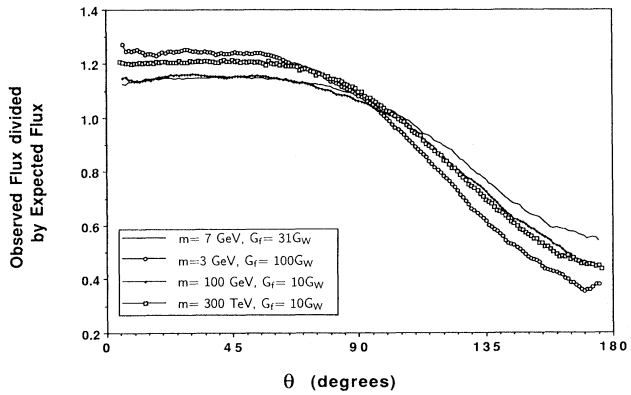

FIG. 5. Sample calculations of the flux of scattered CDM particles normalized to the flux without scattering for four values of mass and coupling constant. The expected flux is defined as the total flux in the absence of scattering in the Earth.

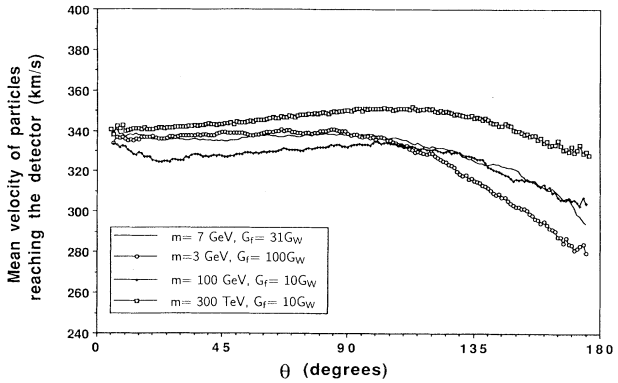

FIG. 6. Sample calculations of the mean velocities of scattered CDM particles for the same parameters as those in Fig. 5. The statistical fluctuations in similar figures in Refs. [11] and [34] have disappeared with an increase in the magnitude of the Monte Carlo simulation.

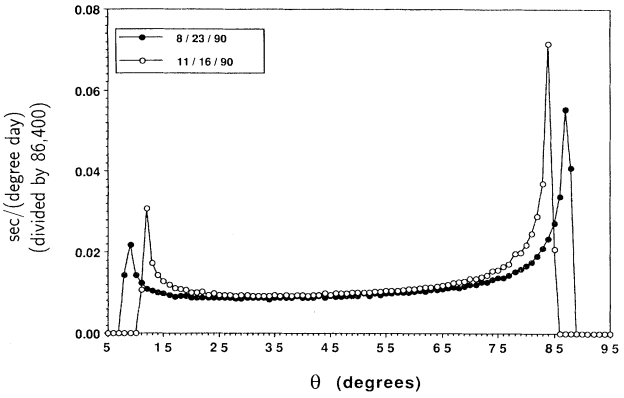

FIG. 8. A plot of the time spent at each possible value of θ for the Ge detector in the Canfranc tunnel in Spain. Two arbitrary dates were chosen to demonstrate the variation with the time of the year.

practical method of searching data for the effects of diurnal modulations due to scattering of CDM particles in the Earth. We propose one such scheme below.

The data from an actual detector come in the form of an energy spectrum which is time tagged to a fraction of a second [33]. The time of each event can be correlated to a unique isodetection ring and, hence, a specific value of θ. One must carefully calculate the time a given detector spends in each 1° interval of θ, so that various bands of θ can be properly normalized to the correct equivalent "exposure time" before direct comparison. Figure 8 shows the time in seconds per degree per day, in units of 86 400 seconds, that the COSME detector at Canfranc, Spain [33] spent at each value of θ for two intervals of time in 1990. Failure to account carefully for this effect will introduce an artificial diurnal modulation.

When the spectrum is separated into two parts, each representing a range of θ where the expected Earth scattering effects are maximally different, we can form the residual spectrum R_i as follows:

$$R_i \equiv N_i(\Delta\theta_1) - N_i(\Delta\theta_2) \ , \tag{5}$$

where $N_i(\Delta\theta_{1,2})$ represents the number of events at energy bin i recorded while the detector was in the chosen band $\Delta\theta_{1,2}$. These quantities must be carefully normalized as discussed above. Each value $R_i \pm \delta R_i$ will be zero, within expected statistical fluctuations, in the absence of CDM elastic scattering in the Earth. If CDM particles do exist with masses and coupling constants that lead to even small diurnal modulations, the experimental residual spectrum R_i will show a deviation from zero which varies with energy bin index i. The value of the mass and coupling of the CDM particle will uniquely determine the precise value of R_i. This test can be applied to the data from any detector that yields an energy spectrum that can be associated with the scattering of CDM particles or with background.

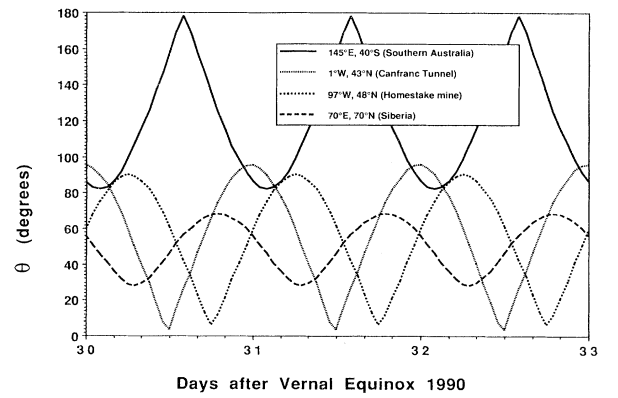

FIG. 7. Plots of detector location using the geometry defined in Fig. 1 over a three-day period in 1990 for four chosen geographical points. Reference to Figs. 5 and 6 demonstrates immediately the advantage of locating the experiment at southern latitudes.

If such an effect were discovered, similar effects could be modeled for various values of $(G_f/G_W)^2$ and $m_\delta c^2$, and compared to the experimental residual spectrum to deduce a probable scenario for CDM. While failure to observe a nonzero residual spectrum would simply improve the exclusion limits for some CDM candidates, its appearance could constitute enough evidence for a claim of positive detection. This analysis has been applied to the data from the COSME germanium (WIMP) detector in Canfranc, Spain [34]. It is clear from the earlier discussions that the geographical location of this detector is far from optimum for collecting data for the purpose of searching for diurnal modulations.

Figure 9 shows the percent daily variation in detection rates for two low energy deposition regions in a Ge detector at an optimum geographical location, for a wide range of $m_\delta c^2$ and $(G_f/G_W)^2$. These include particles ranging from very weakly coupled neutralinos to very

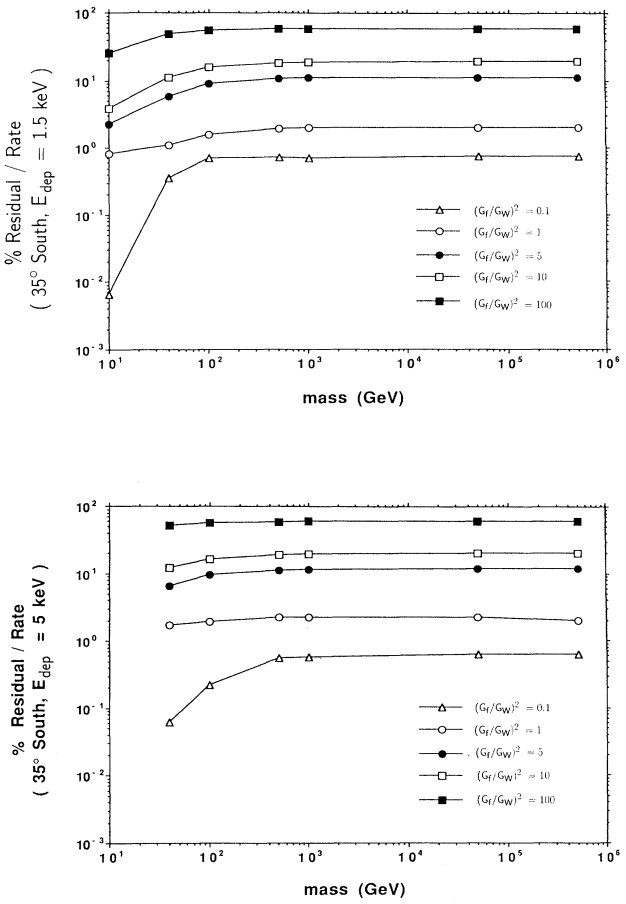

FIG. 9. Calculated percent daily variation in detection rates for a Ge detector, plotted against mass for 5 coupling constants. The detector is located at approximately 35° south latitude. Numerical values are found in Tables II and III.

strongly coupled U(1)′ candidates [35], including heavy Dirac neutrinos. Tables II and III give numerical values for these calculations. Tables IV and V contain values of the expected residual spectra R_i for the same group of candidates.

It is important to realize that if we simply improve the background in an experiment not sensitive to modulations of any type, we can only place bounds on various CDM candidates. These will slowly approach some asymptotic limit that depends on the level of background. It will not improve the bound significantly to continue to run the experiment beyond this point. The bound on the counting rate due to dark matter will be that of unidentified background. In the case that the Earth causes a measurable daily modulation, the sensitivity of the residual spectrum technique will continue to increase with the addition of new data or detector mass, since the growth of R_i is proportional to Nt, while δR_i grows as $\sqrt{Nt}$ (Nt is the usual notation that expresses the magnitude of one such experiment as the product of the number of target nuclei of the detector times the data collection time).

Figure 10 shows the results of a Monte Carlo simulation of residual spectra for two different particle candidates interacting with a Ge detector placed at an optimum geographical latitude (35°–40° S) for the observation of the effect. The simulated background is at levels that have already been achieved in existing detectors. It is important to stress that for the detector modeled, this background level would not allow us to reject either particle using the conventional exclusion methods aforementioned [12–14]. We find that for $m_\delta c^2 > 100$ GeV and after a data acquisition period of $Nt = 2$ kg y, the sensitivity of a diurnal modulation search using a Ge detector at 40° S greatly exceeds that of a conventional search using the same detector [36]. It is clear that CDM consisting of heavy Dirac neutrinos, with masses large enough

TABLE II. Percent daily fluctuation in the detection rates for WIMP's at $E_{\rm dep} = 1.5$ keV due to scattering in the Earth. These values are for a Ge detector placed at an optimal geographical location that would allow data collection in the bands $\Delta\theta_1 \in [160°, 180°]$ and $\Delta\theta_2 \in [85°, 100°]$. Such a site exists in Argentina. Columns show the value of the WIMP's mass. Rows correspond to different values of the coupling, in units of $(G_f/G_W)^2$. Figure 9 displays these results.

	10 GeV	40 GeV	100 GeV	500 GeV	1 TeV	50 TeV	500 TeV
$(G_f/G_W)^2 =$ 0.1	0.0064	0.35	0.71	0.72	0.71	0.74	0.75
$(G_f/G_W)^2 =$ 1	0.81	1.11	1.56	1.94	1.98	2.02	2.02
$(G_f/G_W)^2 =$ 5	2.24	5.75	8.99	10.74	10.99	11.13	11.18
$(G_f/G_W)^2 =$ 10	3.80	11.13	15.88	18.39	19.04	19.44	19.50
$(G_f/G_W)^2 =$ 100	25.65	48.64	55.41	58.46	58.51	58.63	58.80

TABLE III. Similar to Table II but for $E_{dep}=5.0$ keV. A 10 GeV WIMP with a maximum velocity of approximately 760 km/sec cannot deposit that much energy in a Ge detector. The variety of energy thresholds and backgrounds in existing Ge detectors has prompted us to perform the calculations at two different values of E_{dep}.

	10 GeV	40 GeV	100 GeV	500 GeV	1 TeV	50 TeV	500 TeV
$(G_f/G_W)^2=0.1$	$E_{max}<5.0$ keV	0.06	0.22	0.55	0.57	0.62	0.63
$(G_f/G_W)^2=1$	$E_{max}<5.0$ keV	1.74	1.92	2.21	2.25	2.25	1.98
$(G_f/G_W)^2=5$	$E_{max}<5.0$ keV	6.57	9.47	11.20	11.48	11.70	11.72
$(G_f/G_W)^2=10$	$E_{max}<5.0$ keV	12.17	16.59	19.06	19.58	20.13	20.16
$(G_f/G_W)^2=100$	$E_{max}<5.0$ keV	51.94	56.77	59.60	59.93	60.65	60.80

TABLE IV. Absolute value of the residual spectrum, R_i at $E_{dep}=1.5$ keV for a Ge detector placed at an optimal geographical location (35°–40° S) to detect the diurnal modulation. The units are in counts/keV/kg day. Columns show the value of the WIMP's mass. Rows correspond to different values of the coupling, in units of $(G_f/G_W)^2$. The choice of bands used to obtain these values of R_i is $\Delta\theta_1\in[160°,180°]$ and $\Delta\theta_2\in[85°,100°]$.

	10 GeV	40 GeV	100 GeV	500 GeV	1 TeV	50 TeV	500 TeV
$(G_f/G_W)^2=0.1$	0.012	0.016	0.015	0.0032	1.5×10^{-3}	3.2×10^{-5}	3.3×10^{-6}
$(G_f/G_W)^2=1$	0.158	0.519	0.33	0.086	0.044	8.9×10^{-4}	8.9×10^{-5}
$(G_f/G_W)^2=5$	2.07	13.12	9.49	2.38	1.22	0.024	2.4×10^{-3}
$(G_f/G_W)^2=10$	7.03	50.81	33.52	8.15	4.23	0.085	8.5×10^{-3}
$(G_f/G_W)^2=100$	474.6	2218.4	1169.4	259.0	129.91	2.58	0.26

TABLE V. Similar to Table IV, but for $E_{dep}=5.0$ keV. A 10 GeV WIMP with a maximum velocity of approximately 760 km/sec is not able to deposit that much energy in a Ge detector.

	10 GeV	40 GeV	100 GeV	500 GeV	1 TeV	50 TeV	500 TeV
$(G_f/G_W)^2=0.1$	$E_{max}<5.0$ keV	0.0012	0.0028	0.0016	8.3×10^{-4}	1.8×10^{-5}	1.8×10^{-6}
$(G_f/G_W)^2=1$	$E_{max}<5.0$ keV	0.34	0.24	0.064	0.033	6.4×10^{-4}	6.4×10^{-5}
$(G_f/G_W)^2=5$	$E_{max}<5.0$ keV	6.41	5.92	1.62	0.84	0.017	0.0017
$(G_f/G_W)^2=10$	$E_{max}<5.0$ keV	23.74	20.75	5.51	2.86	0.058	0.0058
$(G_f/G_W)^2=100$	$E_{max}<5.0$ keV	1013.0	709.7	172.2	87.51	1.76	0.17

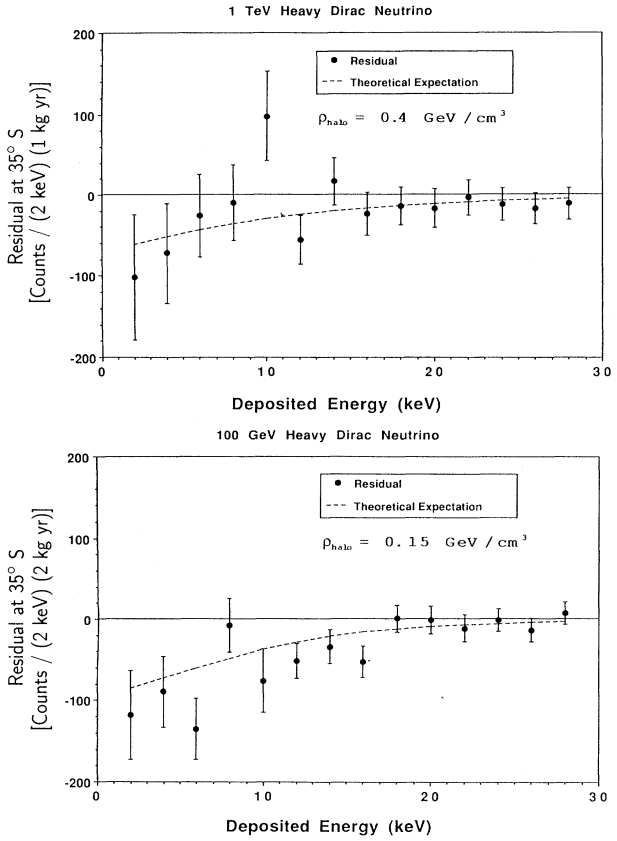

FIG. 10. Simulated experimental residual spectrum for CDM consisting of heavy left-handed Dirac neutrinos (the residual spectrum is the difference between the spectra recorded at two bands or intervals of θ). The detector is taken to be located at 35° south latitude. The choice of bands of θ is as in Table II. Such a selection of the data would make use of approximately 40% of the total collected data. The detector modeled here cannot reject these candidates using conventional exclusion techniques [12–14].

to escape detection by the L3 or ALEPH detectors [37,38], might well be positively identified by a germanium experiment in the southern hemisphere.

Finally, it is obvious by reference to Figs. 2 and 3 that a detector that was able to discriminate between particles coming up from the Earth and those going down into it could detect modulation in the flux and count rate, even when the mass and coupling constant preclude significant scattering in the Earth. This might be feasible in detectors that use the propagation of phonons induced by the coherent collision of a WIMP detected with sensitive thermometry on the surface of the crystal.

IV. SUMMARY AND CONCLUSIONS

It has been demonstrated that for interesting ranges of coupling constants and masses, cold dark matter particles can suffer significant scattering in the Earth. This could result in an experimentally observable modulation of the count rate in many different types of detectors in use or under development. Subtracting properly time-normalized energy spectra from different times of the day could result in a significant increase in sensitivity for placing bounds on particles with certain interesting ranges of coupling strengths and masses. A "real effect" would result in a cumulative residual spectrum that would continue to increase, not asymptotically. It is also clear that detectors that can differentiate particles traveling up from those traveling down could be sensitive to a broader spectrum of CDM mass and coupling constant. Diurnal modulations appear to be a potentially powerful tool for dark matter searches, one that has not yet been exploited.

ACKNOWLEDGMENTS

The authors would like to express their gratitude to Leo Stodolsky and Shmuel Nussinov for very helpful conversations during the early stages of this work. One of us (J.I.C.) would also like to express his deep appreciation to Professor Angel Morales for constant advice and for hosting his stay at the University of Zaragoza at the start of his work on dark matter. The authors are members of the Pacific Northwest Laboratory/University of South Carolina/University of Zaragoza, COSME/TWIN Collaboration, searching for cold dark matter with underground detectors. This work was supported by the National Science Foundation under Grant No. PHYS-9007847.

[1] F. Zwicky, Helv. Phys. Acta **6**, 110 (1933).
[2] S. M. Faber and J. S. Gallagher, Annu. Rev. Astron. Astrophys. **17**, 135 (1979).
[3] Joel R. Primack, David Seckel, and Bernard Sadoulet, Annu. Rev. Nucl. Part. Sci. **38**, 751 (1988), and references therein.
[4] B. Sadoulet, in *TAUP '91,* Proceedings of the Second International Workshop on Theoretical and Phenomenological Aspects of Underground Physics, Toledo, Spain, 1991, edited by A. Morales, J. Morales, and J. A. Villar [Nucl. Phys. B (Proc. Suppl.) **28A**, 3 (1992)].
[5] David N. Schramm, in *TAUP '91* [4], p. 243.
[6] Graciela B. Gelmini, in *TAUP '91* [4], p. 254.
[7] Vera C. Rubin, in *Highlights of Modern Astrophysics, Concepts and Controversies,* edited by Stewart L. Shapiro and Saul A. Teukolsky (Wiley, New York, 1986).
[8] G. F. Smoot *et al.*, Astrophys. J. **396**, L1 (1992).
[9] C. L. Bennett *et al.*, Astrophys. J. **396**, L7 (1992).
[10] E. L. Wright *et al.*, Astrophys. J. **396**, L13 (1992).
[11] J. I. Collar and F. T. Avignone III, Phys. Lett. B **275**, 181 (1992).
[12] S. P. Ahlen, F. T. Avignone III, R. L. Brodzinski, A. K.

Drukier, G. Gelmini, and D. N. Spergel, Phys. Lett. B **195**, 603 (1987).
[13] D. O. Caldwell, R. M. Eisberg, D. M. Grumm, M. S. Witherel, B. Sadoulet, F. S. Goulding, and A. R. Smith, Phys. Rev. Lett. **61**, 510 (1988).
[14] D. O. Caldwell *et al.*, Phys. Rev. Lett. **65**, 1305 (1990).
[15] A. K. Drukier and L. Stodolsky, Phys. Rev. D **30**, 2295 (1984).
[16] M. W. Goodman and E. Witten, Phys. Rev. D **31**, 3059 (1985).
[17] R. L. Mössbauer, J. Phys. G **17**, S1 (1991).
[18] N. E. Booth *et al.*, Nucl. Instrum. Methods **A315**, 201 (1992).
[19] G. Meagher *et al.*, in *Proceedings of the Fourth Workshop on Low Temperature Detectors for Neutrinos and Dark Matter,* Oxford, England, 1991, edited by N. E. Booth and G. L. Salmon (Editions Frontieres, Gif-sur-Yvette, France, 1992), p. 47.
[20] B. Cabrera, B. L. Dougherty, K. D. Irwin, A. T. Lee, J. G. Pronko, and B. A. Young, in *TAUP '91* [4], p. 449; H. Kraus *et al.*, Nucl. Instrum. Methods **A315**, 213 (1992).
[21] A. K. Drukier, K. Freese, and D. N. Spergel, Phys. Rev. D **33**, 3495 (1986).
[22] K. Freese, J. Frieman, and A. Gould, Phys. Rev. D **37**, 3388 (1988).
[23] D. N. Spergel and W. H. Press, Astrophys. J. **294**, 663 (1985).
[24] A. K. Drukier, F. T. Avignone III, R. L. Brodzinski, J. I. Collar, G. Gelmini, H. S. Miley, A. Morales, J. H. Reeves, and D. Spergel, in *TAUP '91* [4], p. 293.
[25] K. Griest, Phys. Rev. D **38**, 2357 (1988).
[26] K. Griest, Phys. Rev. Lett. **61**, 666 (1988).
[27] G. Gelmini, P. Gondolo, and E. Roulet, Nucl. Phys. **B351**, 623 (1991).
[28] D. Mihalas and J. Binney, *Galactic Astronomy* (Freeman, San Francisco, 1981).
[29] G. C. Brown and A. E. Mussett, *The Inaccessible Earth* (Allen and Unwin, London, 1981).
[30] M. H. P. Bott, *The Interior of the Earth* (Elsevier, Amsterdam, 1982).
[31] F. D. Stacy, *Physics of the Earth,* 2nd ed. (Wiley, New York, 1977).
[32] J. I. Collar, Ph.D. thesis, University of South Carolina, 1992.
[33] E. Garcia *et al.*, in *TAUP '91* [4], p. 286.
[34] J. I. Collar *et al.*, in *TAUP '91* [4], p. 297.
[35] D. E. Brahm and L. J. Hall, Phys. Rev. D **41**, 1067 (1990).
[36] J. I. Collar *et al.*, in *Proceedings of the XV International Conference on Neutrino Physics and Astrophysics,* Granada, 1992 [Nucl. Phys. B (Proc. Suppl.) (to be published)].
[37] L3 Collaboration, B. Adeva *et al.*, Phys. Lett. B **231**, 509 (1989).
[38] ALEPH Collaboration, B. Decamp *et al.*, Phys. Lett. B **231**, 519 (1989).